LIGNIN VALORISATION FOR THE ADSORPTION OF Mo(VI) IONS FROM CONTAMINATED MEDIA: A SUSTAINABLE AND ECO-FRIENDLY APPROACH

ELENA UNGUREANU,[*] BOGDAN-MARIAN TOFĂNICĂ,[*] CARMEN O. BREZULEANU,[*] COSTEL SAMUIL,[*] OVIDIU C. UNGUREANU,[**] MARIA E. FORTUNĂ,[***] RĂZVAN ROTARU,[***] STEJĂREL BREZULEANU[*] and VALENTIN I. POPA[****]

[*] *"Ion Ionescu de la Brad" Iasi University of Life Sciences, 3 Mihail Sadoveanu Alley, Iasi 700490, Romania*
[**] *"Vasile Goldis" Western University of Arad, 94 The Boulevard of the Revolution, Arad 310025, Romania*
[***] *"Petru Poni" Institute of Macromolecular Chemistry, 41A Grigore Ghica Voda Alley, Iasi 700487, Romania*
[****] *"Gheorghe Asachi" Technical University of Iasi, 73 Prof. dr. docent Dimitrie Mangeron Alley, Iasi 700050, Romania*
✉ *Corresponding authors: B-M. Tofănică, bogdan.tofanica@iuls.ro*
O. C. Ungureanu, ungureanu.ovidiu@uvvg.ro

Received January 16, 2026

Lignin has a three-dimensional amorphous network structure and hydrophilic functional groups, which make it suitable for the removal of Mo(VI) ions from contaminated aqueous environments. The optimal adsorption conditions were previously established by performing a series of experiments. These experiments targeted the mass of lignin (the adsorbent), the concentrations of Mo(VI) in aqueous environments, the initial pH of the aqueous solution of molybdenum and lignin, and the interphase contact time. In this work, Sarkanda grass lignin was evaluated as an adsorption material for Mo(VI) through a series of characterization analyses, including energy dispersive X-ray spectroscopy (EDX), scanning electron microscopy (SEM), Fourier transform infrared spectroscopy (FTIR), thermogravimetric (TG) and derivative-thermogravimetric (DTG) analyses. The state of chemical equilibrium was described by evaluating several thermodynamic parameters, including enthalpy, entropy, Gibbs free energy, and experimental adsorption isotherms. These parameters were interpreted using the Freundlich and Langmuir models. The kinetics of the process were explained by applying the Lagergren I and Ho-McKay II mathematical models. The assessment of biostability was conducted through the implementation of germination tests on white cabbage seeds (late variety – *Brassica oleracea* L. *var. Capitata alba*). These seeds were introduced into lignin that had been contaminated with Mo(VI), and the filtrates resulting from phase isolation were also examined. The data obtained suggest the potential application of Sarkanda grass lignin in the adsorption of Mo(VI) from aqueous media within the established experimental parameters. This analysis underscores several salient advantages, including the favorable mass ratio and interphase time, a straightforward working technique, the abundance and regenerability of the resource, its economic viability, and its biocompatibility.

Keywords: Mo(VI) ions, lignin, contaminated media, *Brassica oleracea* L., adsorption

INTRODUCTION

Heavy metals are well-known environmental pollutants because of their toxicity, longevity in the environment, and ability to bioaccumulate in living systems. These elements can be lethal to humans and other organisms exposed to them through the food chain, becoming particularly dangerous when mixed with different environmental elements (water, soil, and air).[1]

The removal of heavy metals from contaminated environments, such as aqueous solutions, is necessary because of their frequent occurrence in the waste streams generated by many industries, including electroplating, metal finishing, metallurgy, tanning, chemical production, mining, or battery manufacturing.[2]

Molybdenum is a metal that does not occur naturally in pure metallic form, but in the form of compounds. Thus, almost all exposure is to a molybdenum compound (the most common forms used commercially and found in the environment are molybdenum trioxide and molybdate salts: sodium

molybdate or ammonium molybdate) and not to the metal itself.[3] Molybdenum, a transition metal, exhibits a wide range of oxidation states, ranging from -2 to +6. However, the most stable compounds of molybdenum are those in which the metal is hexavalent.[4]

Acute molybdenum toxicity is a rare occurrence, but it has been documented in cases of exposure to industrial mining and metal processing. Additionally, the discharge of wastewater from industrial processes, which may contain elevated concentrations of molybdenum, can contaminate water or soil, particularly if improper management practices are in place.[5,6] Molybdenum is recognized as a vital dietary micronutrient, but excessive ingestion can result in various health complications, including gout-like symptoms, liver and kidney damage, anemia, bronchitis, gastrointestinal disorders, hypothyroidism, bone and joint deformities, and sterility. In light of these concerns, the World Health Organization (WHO) has established a recommended limit of 70 µg/L Mo in drinking water.[6] Molybdenum is an essential trace element for both plants and animals, functioning as an enzyme activator that promotes optimal growth and development. However, it is crucial to maintain a balanced concentration of molybdenum within living systems. Excessive presence of molybdenum can act as a disruptive factor, particularly in animals. In such cases, the consequences of molybdenosis can be severe, potentially resulting in death.[7]

Recent literature documents a 6% annual increase in global molybdenum production in recent years, attributable to a high demand from the industrial sector and the geopolitical situation. China is the dominant producer, with 110.000 tons, followed by Peru (41.000 tons) and Chile (38.000 tons).[8] The strategic importance of molybdenum stems from its use in high-performance alloys (75% of global consumption is linked to steel production), energy infrastructure (its role in wind turbine shafts and solar panel supports aligns with the energy transition), and missile and armor systems in the defense industries (the “cornerstone of modern manufacturing”). [8,9]

Currently, adsorption is considered a promising technique for the removal and isolation of metal ions from aqueous media. Its efficiency depends on several factors: the amount, surface composition, physicochemical characteristics of the adsorbent, and the chemical nature and concentration adsorbate.[10,11] The most critical step in the adsorption process is the selection of an adsorbent with high adsorption capacity, abundance, and low cost. This adsorbent must not produce secondary pollution, be environmentally friendly, and be renewable.[12-14]

Lignin, the second most abundant natural aromatic polymer in nature, is a material of significant interest due to its abundance and environmental impact. Its annual production from the pulp and paper industry exceeds 70 million tons, and experts project that this figure will reach 225 million tons by the year 2030.[15] Traditionally regarded as a byproduct of agriculture, lignin possesses notable advantages, including its capacity for regeneration, degradation, and non-toxicity. These properties position it as an emerging and promising adsorbent for wastewater remediation.[13-15] Additionally, lignin is rich in active groups, such as phenolic hydroxyl and carboxyl, which facilitate the adsorption of pollutants, including heavy metals and antibiotics.

Traditional lignins derived from softwoods (predominantly guaiacyl-rich) and hardwoods (guaiacyl-syringyl-rich) have been extensively studied, but non-woody grass lignins present distinct chemical and physical advantages that make them superior candidates for specific adsorption applications.[16] The current study selected Sarkanda grass (*Tripidium bengalense*) lignin due to its unique structural and ecological profile. Chemically, grass lignin is an H-G-S (p-hydroxyphenyl-guaiacyl-syringyl) polymer that inherently contains abundant pendant hydroxycinnamic acids–primarily ferulic and p-coumaric acids-attached via ester linkages.[10,14] This unique architectural feature provides a significantly higher density of surface-active phenolic hydroxyl and carboxyl groups compared to heavily cross-linked woody lignins, thereby enhancing its capacity to form stable complexes with target pollutants like Mo(VI). Furthermore, grass lignins generally exhibit a lower degree of carbon-carbon condensation, resulting in a more open and flexible three-dimensional network that favors intrapore adsorbate diffusion.[10,14] From an environmental perspective, Sarkanda grass is a fast-growing, renewable agricultural biomass. Valorizing its lignin not only maximizes adsorption efficiency, but also perfectly aligns with the principles of the circular bioeconomy by circumventing the deforestation associated with traditional timber processing.[16]

As indicated in existent literature, correct interpretation and understanding of adsorption isotherms is imperative for the advancement of the field in general and for the efficient design of adsorption systems in particular.[16,17] In recent years, linear regression analysis has emerged as a predominant tool

for determining the most suitable adsorption models. This method is characterized by its ability to quantify the distribution of adsorbates, systematically analyze the adsorption system, and validate the theoretical assumptions underlying the adsorption isotherm model.[18] The Langmuir isotherm, applicable for monolayer adsorption on a homogeneous site, and the Freundlich isotherm, valid for multilayer adsorption on heterogeneous sites, are the most common models used to estimate the adsorption efficiency as a function of the amount of adsorbent, the initial concentration of the pollutant species, the interphase contact time, or the initial pH of the aqueous solution.[14,18,19]

The kinetics of adsorption are analyzed using mathematical models that accurately reproduce the mechanism by which pollutants are retained on the adsorption substrate.[20] The first-order Lagergren and second-order Ho-McKay kinetic models are applied to a wide range of adsorption systems, from biomass to nanomaterials as an adsorbent and from heavy metals to pharmaceuticals as an adsorbate or contaminant. These models focus on the mechanism by which the adsorbate diffuses from the aqueous environment to the active centers on the surface of the adsorbent.[21]

The current study evaluates the static adsorption of Mo(VI) from aqueous environments on Sarkanda grass lignin using surface, spectral, and thermogravimetric analyses, as well as thermodynamic, kinetic, and biological parameters. The study recommends the biomass fraction as a sustainable alternative under precisely established experimental conditions.

EXPERIMENTAL

Materials and methods

Sarkanda grass lignin extracted from *Tripidium bengalense* plants was offered by Granit Récherche Development S.A., Lausanne, Switzerland.[14] $Na_2MoO_4 \cdot 2H_2O$ was supplied by ChimReactiv S.R.L., Bucharest.

Brassica oleracea L. seeds (*Capitata alba* var., vegetation period of 100-110 days from transplanting) offered by "Ion Ionescu de la Brad" Iasi University of Life Sciences, Iasi, Romania.

Adsorption experiments

The effectiveness of the process, known as adsorption, is conditioned by several variables. These include the quantity of the adsorbent employed, the initial pH of the aqueous solution, the concentration of the pollutant, and the duration of the reaction.[22,23] To ensure optimal experimental conditions, preliminary tests were conducted.

Then, a 5 g aqueous solution of Sarkanda grass lignin/L was selected to ensure the presence of an adequate number of active adsorption centers within the structure of the adsorption substrate.[13] Complexation is one of the primary mechanisms by which lignin eliminates heavy metals, the main functional groups in its structure (phenolic hydroxyl, carbonyl, and carboxyl) facilitating the formation of stable complexes of Mo(VI).[24,25] Experimental tests recommend a pH of 5.7, as at a low pH, the presence of excess protons can compete with Mo(VI) ions for the available lignin binding centers, and at a pH above 5.7, the possibility of precipitation of the metal ion appears, with adsorption being diminished or even blocked.[25,26]

The stock solutions of metal ion in a concentration of 1000 mg/L were prepared by separately dissolving $Na_2MoO_4 \cdot 2H_2O$ in distilled water. The working solutions were prepared by diluting with distilled water an exact volume measured from the stock solutions. The concentrations of metal ions in aqueous media (mg/mL) are as follows: 9.594, 19.188, 28.782, 38.376, 47.970, 57.564, 67.158, 76.752, 86.346, 95.94. In the experiment, 20 milliliters of a solution containing $Na_2MoO_4 \cdot 2H_2O$ at a designated concentration was added to each sample of Sarkanda grass lignin. The samples were then allowed to stand under controlled laboratory conditions for three distinct contact times: 30 minutes, 60 minutes, and 90 minutes. The rationale for this design was to identify the optimal adsorption time for Mo(VI). It was hypothesized that this time period would directly correlate with achieving chemical equilibrium.

Spectrophotometric determination of Mo(VI)

The concentration of Mo(VI) was determined by employing the ammonium thiocyanate method, with absorption measured at 565 nm.[27] Quantitative determination of the Mo(VI) obtained after filtration from the aqueous media was carried out by analysis of a precisely measured volume (2 mL) according to the experimental procedure, and the concentration value for each sample was calculated from the regression equation of the calibration curve.

For the analysis, we used a laboratory UV-vis spectrophotometer, model VS721N, with a wavelength range of 300-1000 nm, manufactured by JKI in Shanghai, China.

Isotherm models

Adsorption isotherm models establish correlations between the performance of the adsorbent and the adsorbate as a function of specific experimental parameters (pH, temperature, concentration range of interest for the adsorbent and adsorbate).[28] Moreover, they furnish indications concerning the potency of the adsorbent-

adsorbate interactions, the maximum adsorption capacity, as well as information regarding the characteristics of the adsorbent (*e.g.*, specific surface area or pore size distribution).[28] The utilization of analytical Langmuir and Freundlich isotherm models is a prevalent practice in the modeling of adsorption data sets across a myriad of studies, encompassing the retention of metal ions, dyes, pharmaceuticals, and select categories of organic pollutants.[28,29]

The adsorption capacities of Mo(VI) were determined according to the following Equation (1):[10]

$$q = (C_i - C_e)V/m, \text{ (mg/g)} \quad (1)$$

where C_i – initial concentration (mg/mL); C_e – equilibrium concentration (mg/L); V – volume of molybdenum ion solution (L); m – mass of Sarkanda grass lignin (g).

The Langmuir-Freundlich isotherm is a theoretical framework that elucidates the monolayer adsorption of a single substance on heterogeneous surfaces, such as that of Sarkanda grass lignin. It describes the quasi-Gaussian asymmetric distribution of adsorption energies on the heterogeneous surface of the adsorbent.[30]

The Langmuir Equation can be written in the following linear form (2):[10]

$$C_e/q_e = 1/q_m \cdot k_L + C_e/q_m \quad (2)$$

where q_e is the amount of ions adsorbed per unit of mass of lignin (mg/g) at equilibrium; q_m is the maximum amount of molybdenum ions retained on the absorbent after saturation (mg/g); K_L is the Langmuir constant (L/mg); C_e is the equilibrium concentration of molybdenum ions in solution (mg/L).

The linear form of the Freundlich isotherm is as follows: [10]

$$\log q_e = \log k_F + 1/n \cdot \log C_e \quad (3)$$

where k_F – Freundlich constant, indicating adsorption capacity; n – constant characterizing the affinity of molybdenum ions to sorbent/lignin; q_e – amount of molybdenum ions adsorbed per unit of weight of lignin (mg/g) at equilibrium; C_e – concentration at the equilibrium of molybdenum ions in solution (mg/L).

The interpretation of experimental data is based on the correlation coefficients (R^2) calculated by the least squares method, whose values highlight the most appropriate applicable model.[14,18]

Thermodynamic studies

The thermodynamic behavior of adsorption was assessed based on van't Hoff's laws, which enabled the calculation of thermodynamic parameters (free energy change [ΔG], enthalpy [ΔH], and entropy [ΔS]). These parameters are capable of providing information on the spontaneity and energetic nature of adsorption. These attributes are essential for evaluating the efficiency of adsorption and guiding its scalability.[31]

Kinetic models

Kinetic modeling is vital for characterizing safe, environmentally friendly, and cost-competitive adsorption processes, providing essential information about the rate and mechanism of adsorption, two key factors for process optimization.[32] The most common kinetic models used to monitor the kinetics of adsorption processes are the first-order Lagergren model and the second-order Ho-Mc Kay model.[33]

The Lagergren model finds application in the domain of liquid-solid adsorption, and its mathematical expression is given by Equation (4):[10]

$$\ln [q_e/(q_e - q)] = k_1 \cdot t \quad (4)$$

The equation of the Ho and McKay model reflects the adsorption capacity of the solid phase[34] and is expressed through the following relationship:[10]

$$t/q_t = (1/k_2 \cdot q_e^2) + t/q_e \quad (5)$$

where k_1, k_2 – constant adsorption rates for model 1 and 2; respectively; q_e, q_t – adsorption capacity at equilibrium and at time t, respectively.

Linear regression facilitated the selection of the most appropriate kinetic model for the evaluation of the experimental data.[10]

Surface characterization

The use of spectroscopy (Fourier-transform infrared, FTIR) facilitates the identification of distinctive molecular “fingerprints”, rendering it an optimal technique for the determination of chemical structures, the analysis of mixtures, and the assessment of quality control. The analysis was conducted on potassium bromide pellets utilizing a Bruker Vertex 70 spectrometer, with a resolution of 2 cm^{-1}.[35]

Scanning electron microscopy (SEM) was conducted using a Quanta 200 microscope (operated at 5 kV), manufactured in Brno, Czech Republic. This high-resolution technique enables detailed morphological characterization of materials at both nanometric and micrometric scales.[36]

Energy-dispersive X-ray spectroscopy (EDS) enables essential qualitative and semi-quantitative elemental analysis of materials, offering compositional insights that are typically unattainable through conventional laboratory techniques.[20]

Thermal analyses

Thermal stability is directly correlated with the kinetics of a process and the sorption capacity of a polymer, such as lignin. The evaluation of these phenomena was performed by conducting thermogravimetric (TG) and differential thermogravimetric (DTG) analyses using the STA 449F1 Jupiter equipment (Netzsch Company, Selb, Germany). The thermal behavior of the samples was evaluated according to the percentage mass loss from ambient temperature to 700 °C at a heating rate of 10 °C/min in an inert nitrogen atmosphere.[37]

Biological experiments

The adsorption capacity of Sarkanda grass lignin for Mo(VI) from aqueous media was also analyzed from a biological point of view by performing germination tests on *Brassica oleracea* L. seeds (*Capitata alba* variety). These tests were conducted on lignin contaminated with Mo(VI) and on the filtrates resulting from phase isolation. Distilled water was utilized as a control sample for the filtrates, while uncontaminated adsorbent was employed for the contaminated lignin. The experiment was conducted over a period of seven days under controlled laboratory conditions (20 °C ±1, 15 hours of light/9 hours of dark). The experiment was replicated three times, with each replicate consisting of 20 seeds. The seeds were initially disinfected for five minutes in 5% sodium hypochlorite (NaClO) and then washed three times with Milli-Q ultrapure water to mitigate a specific odor.[20] The seeds were then introduced into test tubes (180 x 18 mm) for incubation for one hour with intermittent shaking to allow soaking in filtrates and distilled water. Following this, the seeds were distributed uniformly in Petri dishes (90 x 15 cm) and two overlapping filter paper discs were attached.[14] Seeds that were swollen, rotten, or moldy at the end of the germination period were considered ungerminated, as recommended by the methodology. The phytotoxicity of filtrates and lignin contaminated with aqueous Mo(VI) solutions was investigated.[38] The following experiment was conducted in the concentration range of 9.594 to 95.94 milligrams per milliliter, at three distinct interphase contact times. The energy and germination capacity of each sample was determined, and the relevant formulas (6) and (7) were applied to calculate the values.[10]

$$E_g = (a/n) \cdot 100 \quad (6)$$

$$F_g = (b/n) \cdot 100 \quad (7)$$

where a is the number of seeds germinated after three days, n is the total number of seeds analyzed, b is the number of seeds germinated at the end of the period (seven days).

RESULTS AND DISCUSSION

Influence of experimental parameters on Mo(VI) adsorption on Sarkanda grass lignin

Initial concentration of Mo(VI)

The amount of metal ion retained per unit mass of adsorbent (q, mg/g) is a critical indicator of adsorption performance, contingent on its concentration in the aqueous medium.[39] Theoretically, an increase in the proportion between the initial number of moles of Mo(VI) and the number of active adsorption centers of Sarkanda grass lignin should result in an increase in the amount of metal ion retained per unit mass of lignin until saturation. At this point, the lignin pores become partially or totally inaccessible. Irrespective of the increase in contact time, the adsorption becomes passive to blocked.[14,20] Figure 1 reproduces the adsorption capacity of Sarkanda grass lignin at the optimal contact time between phases of 60 minutes. An increase in the lignin adsorption capacity can be observed, from 1.60 mg/g at a concentration of 9.594 mg/L to 13.84 mg/g. mg/g at concentration of 95.94 mg/L. In summary, the observed rise in the concentration of Mo(VI) within the designated concentration range suggests an enhancement in the adsorption capacity of lignin. This phenomenon can be attributed to the strong affinity between Mo(VI) and lignin,[26] thereby validating the tendency of the bioresource to yield stable lignocomplexes following activated adsorption.[39]

Dose of Sarkanda grass lignin

The adsorbent dosage has been demonstrated to exert a significant influence on the process of adsorption. It has been shown to provide valuable hypotheses regarding the potential of a material to adsorb, particularly with regard to the available binding centers for the removal of a particular pollutant species at a given concentration.[40]

In order to ascertain optimal experimental conditions, preliminary tests were conducted within the range of 4–40 g lignin/L of an aqueous Mo(VI) solution, a range that has been recommended in existent literature.[14] As depicted in Figure 2, increasing the lignin dosage did not enhance the adsorption capacity; conversely, it led to a continuous decrease in the amount of Mo(VI) retained per unit mass of adsorbent (mg/g). This inverse relationship is a well-documented phenomenon in solid-liquid adsorption systems, primarily driven by two factors. First, at higher adsorbent dosages, the

excess availability of active binding sites relative to the fixed Mo(VI) concentration results in partial unsaturation of the lignin surface. Second, at elevated concentrations, suspended lignin particles have a high tendency to agglomerate. This particle overlapping reduces the effective surface area, promoting rapid, but strictly superficial complexation. Consequently, the outer layer of the agglomerates becomes saturated and sterically blocks the diffusion of Mo(VI) into the internal porous network, leaving internal functional groups unutilized. To mitigate this superficial blockage and prevent particle agglomeration, maintaining an optimal adsorbent-to-volume ratio is crucial. The experimental data establish that a dosage of 5 g/L provides the ideal balance, minimizing steric hindrance and maximizing pore accessibility, thereby ensuring both the efficient removal of Mo(VI) and the economical utilization of the biomass.

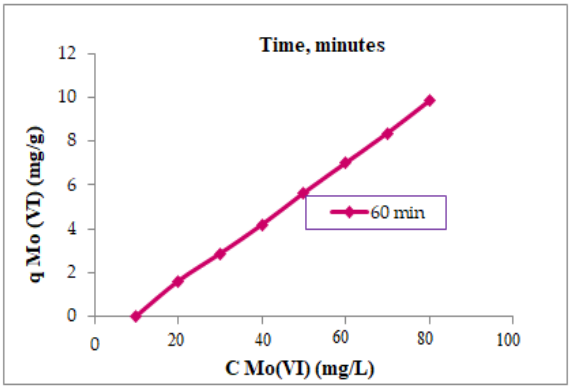

Figure 1: Adsorption capacity of Sarkanda grass lignin at a contact time of 60 min and pH of 5.7

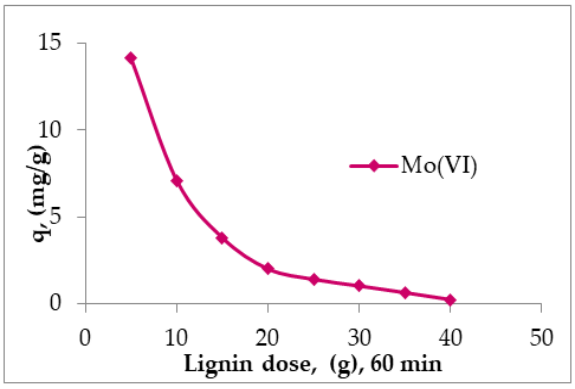

Figure 2: Influence of Sarkanda grass lignin dose on the adsorption of Mo(VI) at a concentration of 95.94 mg/L, at a contact time 60 min, pH 5.7

Contact time

The equilibrium between adsorbent and adsorbate is imperative in the realm of practical applications. According to a previous study, the interphase contact time should be extended to facilitate a more thorough appreciation of the process's kinetics.[41] The objective was to ascertain an optimal contact time for the adsorption equilibrium, and the initial adsorption capacity was evaluated at seven distinct times – 10, 20, 30, 40, 50, 60, and 120 minutes were selected, after which the results obtained were used to select three interphase times – of 30, 60, and 90 minutes, respectively. The experimental data demonstrate that an augmentation in the contact time between Sarkanda grass lignin and the aqueous molybdenum solution results in a more pronounced increase in the amount of Mo(VI) retained during the initial stage. Subsequently, the adsorption becomes inactive. As seen in Figure 3, the adsorption capacity increases rapidly during the initial stages and reaches a maximum at 60 minutes of contact time. Crucially, when the contact time is further extended to 90 and 120 minutes, the kinetic curve exhibits a distinct plateau, indicating no significant change in the amount of Mo(VI) retained. This confirms that the active binding sites are fully saturated and chemical equilibrium has been successfully achieved. Therefore, 60 minutes is definitively established as the optimal adsorption time under these experimental conditions.

Initial solution pH

The pH of the solution and the surface charge of the sorbent are critical factors in the adsorption process of Mo(VI).[42] The molybdate anion, MoO_4^{2-}, is the dominant form of Mo at pH 6. Under moderately acidic conditions, molybdate is protonated into less charged anions ($HMoO_4^-$), and in strongly acidic environments, molybdic acid, $MoO_3(H_2O)_3$, appears.[43] In addition, molybdate is able to form isopolymetalates, such as $Mo_7O_{24}^{6-}$ or $Mo_8O_{26}^{4-}$, at pH levels below 6.[44] Thus, it is anticipated that the molybdate ion will be a predominant substance in solutions in all natural reservoirs.[42] On the other hand, in alkaline environments (pH 9-10), Mo(VI) is fixed and precipitated, which implies the blocking of any possible adsorption.[26] Furthermore, according to existing literature, lignin exhibits optimal adsorption capacity at a pH of 4.0-6.5.[14,31] In light of these findings, preliminary experimental tests were conducted to ascertain the variation of the adsorption capacity of Sarkanda grass lignin depending on the initial pH of the aqueous Mo(VI) solution. The targeted pH range for these tests was

0-7. Figure 4 demonstrates a proportional increase in the adsorption capacity of lignin with increasing pH of the solution of the polluting species. This increase can be attributed to a probable deprotonation of the carboxyl and hydroxyl groups in the lignin structure. These groups became available to associate with Mo(VI), obtaining a maximum (11.98 mg/g) at pH 5.7, which is considered the optimal pH. Irrespective of the initial concentration of the Mo(VI) solution, at a pH higher than 5.7, poorly soluble precipitates resulted, with the lignin particles likely becoming fixation areas for the Mo(VI) ions, located on the surface of the adsorbent.

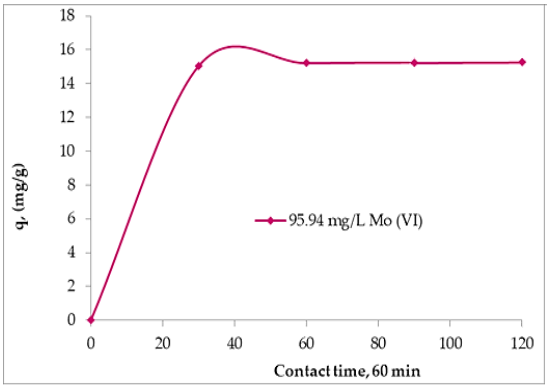

Figure 3: Influence of contact time on the adsorption of Mo(VI) onto Sarkanda grass lignin at pH 5.7

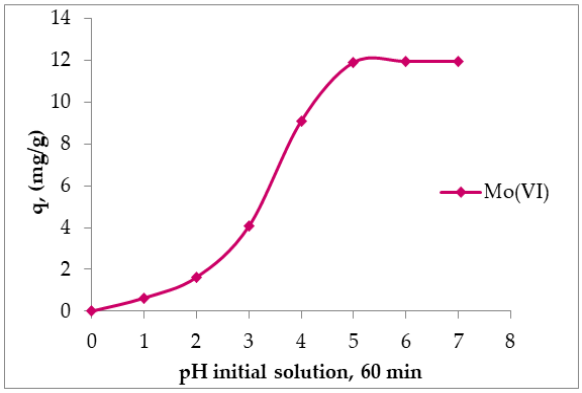

Figure 4: Influence of initial solution pH on the adsorption of Mo(VI) onto Sarkanda grass lignin

Adsorption isotherms

The adsorption equilibrium between the phases involved in the process is interpreted based on experimental adsorption isotherms. These isotherms explain the distribution of the adsorbate between the homogeneous or heterogeneous solid phase, in monolayer or multilayer, and the liquid phase. They also allow the distinction between physiosorption and chemisorption.[45] The modeling of adsorption isotherms is important in evaluating the practical applicability of adsorbents. This modeling is performed with the help of mathematical models capable of reproducing the interactions between adsorbent and adsorbate as faithfully as possible.[46] The Langmuir-Freundlich isotherms are the most applied and useful for analyzing the adsorption equilibrium.[10] The Langmuir isotherm explains monolayer adsorption on an adsorbent with a homogeneous surface and a finite number of adsorption sites without transmigration of the adsorbate in the surface plane.[10,14,47,48] The linear Freundlich isotherm explains monolayer and multilayer adsorption. The phenomenon of heterogeneous surface adsorption, characterized by a disordered distribution of adsorption energy, is of particular interest in this study. The focus is on the adsorption process itself, taking place on an adsorbent surface with a heterogeneous composition.[2,14,49]

The values of the correlation coefficients R^2, deduced from the linear representation of the regression equations for the two models, are indicative of the efficiency and applicability of the process.[2] Consequently, if R^2 has high values, it is considered that the applied model is more adequate in describing the adsorption.[14,50] Figure 5 (a and b) reproduces the linear representation for the Freundlich and Langmuir models of Mo(VI) adsorption from aqueous solutions on Sarkanda grass lignin under experimental conditions established as optimal: temperature of 20±0.1 °C and contact time of 60 minutes, with a pH of 5.7. The results are presented in Table 1, which includes the characteristic indices of the Freundlich (R^2, 1/n, k_F) and Langmuir (R^2, q_m, K_L) models.

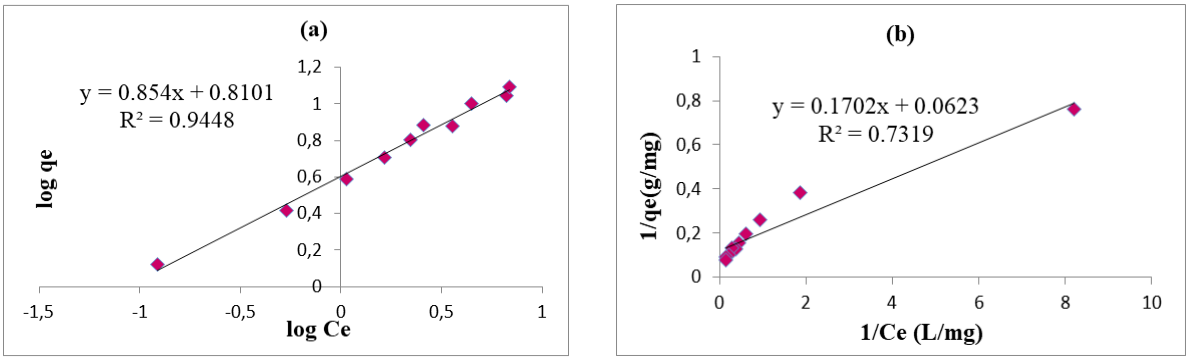

Figure 5: Freundlich adsorption model (a) and Langmuir adsorption model (b) for Mo(VI) adsorption onto Sarkanda grass lignin after 60 min

Table 1
Characteristic parameters of Freundlich and Langmuir models, for Mo(VI) adsorption on Sarkanda grass lignin

Time (min)	Freundlich model			Langmuir model		
	R^2	1/n	k_F	R^2	q_m (mg/g)	K_L
30	0.9365	0.9028	1.9934	0.7126	13.0208	0.0798
60	0.9448	0.9138	1.9762	0.7319	14.7734	0.0766
90	0.9389	0.9287	1.9821	0.6879	14.8104	0.0711

As illustrated in Table 1, the correlation coefficients (R^2) of the Langmuir model range from 0.6879 to 0.7319, indicating a decrease in value compared to the Freundlich model, which ranges from 0.9365 to 0.9448. Consequently, from the perspective of the correlation indices, the Freundlich model is more appropriate for characterizing the retention of Mo(VI) on Sarkanda grass lignin. Furthermore, the low values of the Langmuir constant K_L (0.0711–0.0798) suggest a non-uniform surface of Sarkanda grass lignin and imply that the adsorption process occurs through multilayer formation rather than monolayer coverage. Additionally, the values of K_F (1.9762-1.9934) and 1/n (0.9028-0.9287) are minimal, indicating the presence of binding energy through adsorption resulting from ion exchange interactions or superficial complexation. Consequently, it is not possible to obtain clear information regarding the physical or chemical nature of Mo(VI) adsorption on lignin. This necessitated the thermokinetic interpretation of the process.

Thermodynamic insights

Adsorption thermodynamics provides information about the feasibility of the process, its spontaneous or nonspontaneous character, and its underlying energetic dynamics. These aspects are particularly important in the selection of the adsorbent and in the optimization of experimental conditions, which are essential for the efficiency of adsorption and implicitly for its application extension.[51]

Table 2 reports negative values of the Gibbs free energy (ΔG), ranging from -26.01 to -37.93. These values suggest that the adsorption of Mo(VI) on lignin occurred spontaneously, favorably from a thermodynamic point of view, following a mechanism where electrostatic interactions (ion exchange or hydrogen bonds) predominate over less covalent interactions.[52] Additionally, positive enthalpy values (ΔH) were obtained at both pH values, with variations ranging from 10.95 to 15.48 (see Table 2). These results suggest an endothermic and physical character for the adsorption process. This finding aligns with the literature, which establishes a range of values between 2 and 20 kJ/mol for van der Waals adsorption.[53]

As indicated in Table 2, biosorption cannot be considered physical in nature. However, the probability of ion exchange interactions between Mo(VI) and the functional groups of Sarkanda lignin appears to be significant, thereby explaining the values obtained for both (ΔH) and (ΔG).[14] In summary, the values of the thermodynamic functions are analogous to those observed for high-efficiency absorbers, as previously established,[54] and consistent with the hypotheses derived from the interpretation of the adsorption isotherms.

Table 2
Thermodynamic parameters calculated for the adsorption of Mo(VI) ions from aqueous media onto lignin from Sarkanda grass

Pollutant	pH	Time (min)	ΔG (kJ/mol)	ΔH (kJ/mol)	ΔS (J/mol K)
Mo(VI)	1.89	30	- 26.01	13.17	98.21
		60	- 28.13	10.95	89.01
		90	- 29.04	12.03	92.58
	5.7	30	- 31.18	15.48	110.84
		60	- 34.86	14.56	131.98
		90	- 37.93	14.99	123.56

Adsorption is favored by an increase in temperature (within the stability limits of lignin). This phenomenon can be attributed to the increase in molecular agitation, diffusion, and activation energy required to overcome activation barriers, such as the dehydration of the metal ion or the lignin surface, or for the formation of new chemical bonds.[55] The positive values of the entropy change (ΔS), located in the range of 89.01-131.98, characteristic of the retention of Mo(VI) from an aqueous solution on Sarkanda grass lignin, suggest that the disorder of the system intensifies, most likely as a result of the decrease in the degree of ordering of the solvent molecules around the surface functional groups of lignin.[14]

Kinetic modeling

The design of an efficient adsorption system is contingent upon the adsorption kinetics, which estimate the rate at which the process occurs. This kinetics are influenced by the complexity of the adsorbent surface, the solute concentration, and the flow rate.[56] The literature typically recommends two mathematical models for interpreting the adsorption kinetics: the pseudo-1st order Lagergren model for liquid-solid systems and the pseudo-2nd order Ho-McKay model for estimating the adsorption capacity of the solid adsorption support. The adequacy of any model depends primarily on the level of error, which is assessed by the correlation coefficient (R^2).[21,34,56] Figure 6(a) and (b) illustrate the linear dependence of both models regarding the adsorption of Mo(VI) from an aqueous medium on Sarkanda grass lignin at a normalized initial concentration of 100 mg/mL. Table 3 presents the main kinetic parameters derived from the slopes and intercepts. The ordinate of the linear dependences has been achieved for both kinetic models.

The correlation coefficients (R^2) obtained by linear regression, recorded in the case of the pseudo-I order Lagergren model, show values below 0.8, falling in the range of 0.6781-0.8472 (see Table 3). The low values of the correlation coefficients suggest the probability of electrostatic interactions between Mo(VI) and the free functional groups of Sarkanda grass lignin, as well as the occurrence of a chemisorption that the Lagergren model fails to explain.[14] This limitation restricts the model's involvement in the kinetic interpretation of the studied system. Conversely, the correlation coefficients (R^2), as determined by implementing the Ho-McKay kinetic model, are found to be unity in all instances, as illustrated in Table 3. Furthermore, the other parameters, in this case q_e and K_2, underscore the affinity of Mo(VI) as a pollutant species with Sarkanda grass lignin as an adsorbent. They also highlight the complexation tendency, which is supported by the accessibility of lignin functional groups to participate in activated dative exchanges.[14] These exchanges ultimately lead to the formation of relatively stable lignochelates.[26]

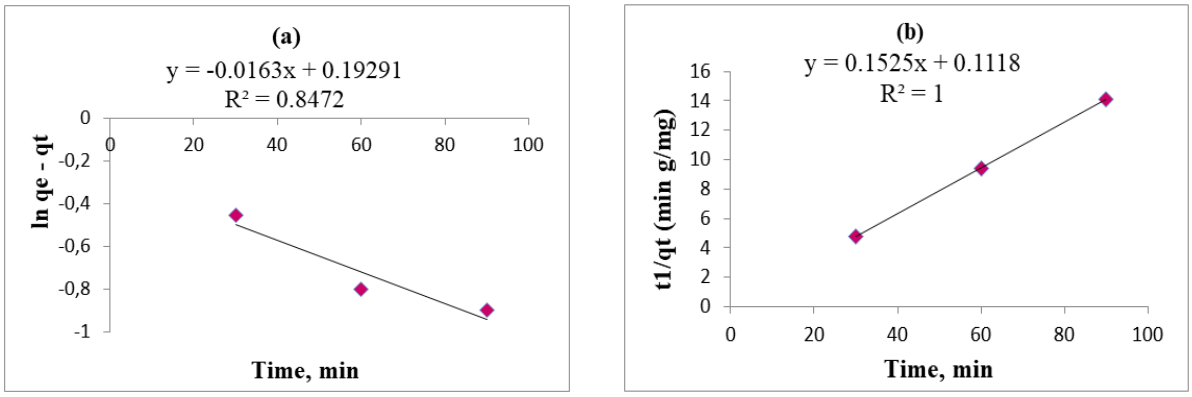

Figure 6: Linear representation of the Lagergren pseudo-I order model (a) and Ho-McKay pseudo-II order model **(**b) for adsorption of Mo(VI) onto Sarkanda grass lignin after 60 min

Table 3
Kinetic parameters of the Lagergren and Ho-McKay models for Mo(VI) adsorption on Sarkanda grass lignin

c_i	Lagergren model			Ho-McKay model		
(mg/mL)	R^2	q_e (mg/g)	K_1 (min^{-1})	R^2	q_e (mg/g)	K_2 (g/mg·min)
10	0.7821	1.3301	-0.0019	0.9942	1.9721	2.3408
20	0.7926	2.0671	-0.0022	0.9918	3.0104	1.8034
30	0.8303	3.2407	-0.0016	0.9975	5.0104	3.0541
40	0.8358	5.0516	-0.0019	0.9994	7.9913	2.9791
50	0.7091	7.2901	-0.0021	0.9961	9.8934	1.9948
60	0.8472	8.2106	-0.0018	0.9952	11.1663	2.0516
70	0.6781	8.2410	-0.0021	0.9937	12.7803	1.3437
80	0.7662	8.9304	-0.0020	0.9981	13.7028	2.8925
90	0.8470	9.0002	-0.0020	0.9924	14.3517	1.6324
100	0.8642	10.6314	-0.0018	0.9968	15.6638	1.3278

The Ho-McKay model is superior to the Lagergren model due to its accuracy[10] and leads to the hypothesis that the kinetics of Mo(VI) adsorption on Sarkanda grass lignin is mainly determined by the chemical interaction between the metal ion and the functional groups in the lignin structure, especially the carboxyl and hydroxyl groups. This suggests the predominance of chemical adsorption over physical adsorption, with possible modifications to the internal structure of lignin, including the cleavage and formation of new bonds.[26]

Surface morphology

In addition to insights derived from equilibrium and thermokinetic modeling, direct surface analysis of Sarkanda grass lignin before and after adsorption can provide valuable information regarding the nature of the interaction between the phases involved in the process.

In order to perform scanning electron microscopy (SEM) analysis, the prepared sample was metallized with platinum (Pt) to increase contrast. As illustrated in Figures 7(a) and 7(b), the morphology of Sarkanda grass lignin was examined before and after the adsorption of Mo(VI) at a concentration of 95.94 milligrams per liter and an interphase contact time of 60 minutes. Figure 7(a) presents a micrograph (SEM) of uncontaminated lignin, highlighting the presence of well-isolated micrometric particle agglomerations (approximately 4 µm) with irregular shapes. These agglomerations exhibit clear differences in morphology compared to the surface of lignin contaminated with Mo(VI), as observed in Figure 7(b). This figure confirms the interaction between the two phases, followed by the diffusion, adsorption, and deposition of Mo(VI) within the porous structure of the lignin. This process results in a modification of the texture and appearance of the lignin.

The employment of EDX analysis yielded unequivocal evidence concerning the adsorption of Mo(VI) within the lignin matrix, as illustrated in Figures 8(a) and 8(b). Consequently, the EDX spectrum of lignin contaminated with an aqueous solution of Mo(VI) at a concentration of 95.94 mg/L, contact time of 60 minutes and a pH of 5.7, showing clear and distinct peaks corresponding to the

Mo(VI) ion (Fig. 8(b)), is distinct from the spectrum of uncontaminated lignin (Fig. 8(a)). This observation confirms the transfer of Mo(VI) from the aqueous phase to the solid lignin adsorbent.

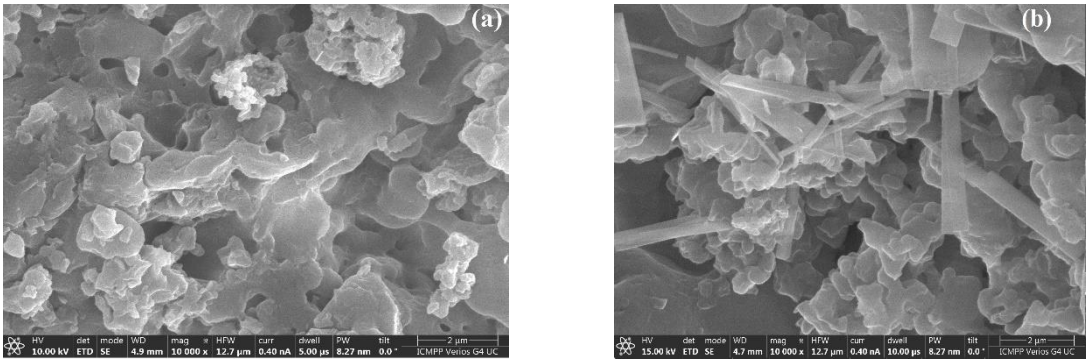

Figure 7: SEM images of Sarkanda grass lignin before adsorption (a) and after Mo(VI) adsorption (b), contact time of 60 min

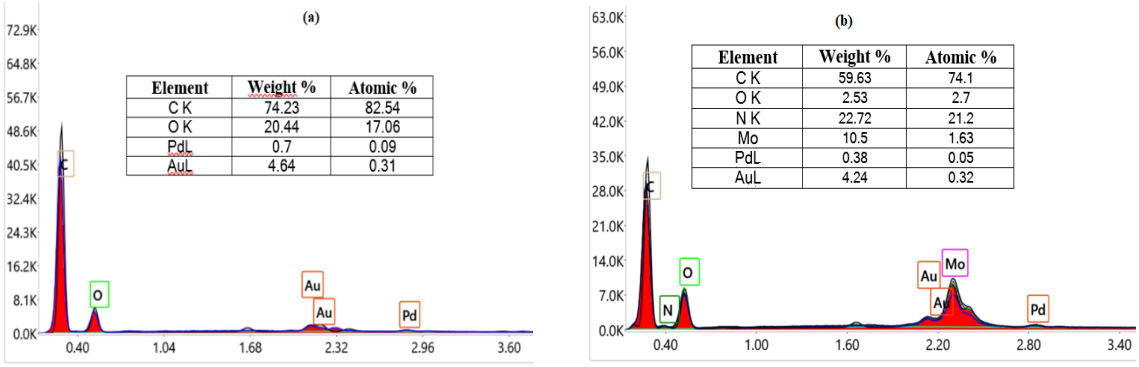

Figure 8: EDX elemental analysis of Sarkanda grass lignin before adsorption (a) and after (b) Mo(VI) adsorption at a contact time of 60 min

FTIR spectroscopy is recognized as a precise and efficient analytical technique frequently utilized in biomolecular research due to its capacity to provide structural and functional information, which is of particular importance for the characterization and identification of complex samples.[57] Figure 9 presents the FTIR spectra for unmodified lignin (UL) and lignin contaminated with Mo(VI) at a concentration of 95.94 mg/L and a contact time of 60 minutes (CL), respectively.

Peaks associated with lignin are observed at 3424 cm^{-1} (hydroxyl groups in phenolic and aliphatic structures), 2919 and 2852 cm^{-1} (CH stretching in aliphatic methylene groups that can originate from fatty acids present in the lignin), 1708 cm^{-1} (C=O stretching, characteristic of the unconjugated carbonyls and the abundant ferulate/p-coumarate ester linkages specific to grass lignins), 1646 cm^{-1} (OH bending of absorbed water), 1601 and 1514 cm^{-1} (aromatic skeleton vibrations), 1461 cm^{-1} (C–H deformation combined with aromatic ring vibration), 1269 cm^{-1} (guaiacyl unit, G ring and C=O stretch), 1218 cm^{-1} (C–O stretching vibrations in phenols), 1150 cm^{-1} (CH in-plane deformation), 817 cm^{-1} (C–H out-of-plane vibrations in position 2, 5 and 6 of guaiacyl units), as illustrated in Figure 9 (UL).[35,58] The spectrum of lignin contaminated with Mo(VI) exhibits peaks that are specific to the two precursors, yet some differences also emerge. Thus, a new vibration appears at 3189 cm^{-1}, which seems to show the formation of a hydrogen bond between the O-H hydroxyl groups in phenolic and aliphatic structures (lignin). C–H out-of-plane vibrations in position 2, 5 and 6 of guaiacyl units of lignin (817 cm^{-1}) migrates in the system spectrum to 807 cm^{-1} and becomes much more prominent, indicating a lower energy value. Furthermore, vibrations at 584 cm^{-1} (Mo–O, stretching bond) are detected (Fig. 9 (CL)).[59] These changes indicate the existence of chemical interactions between lignin and Mo(VI), thus confirming the occurence of adsorption.

Thermostability

As illustrated in Figure 10, the TG and DTG curves were recorded under a nitrogen atmosphere for pristine Sarkanda grass lignin (Fig. 10(a)), and for lignin after contact with an aqueous Mo(VI) solution at a concentration of 95.94 mg/L and a contact time of 60 minutes (Fig. 10(b)). The thermal behavior of all samples was evaluated according to the percentage mass loss from ambient temperature to 700 °C. Mass loss is evident for uncontaminated lignin, with maximum decomposition peaks located at approximately 54, 281, 391, and 438 °C, as illustrated in Figure 10(a). The TG curve documented major mass losses at 92.4 °C (6.34% loss), 411.8 °C (30.39% loss), and 484.3 °C (14.33% loss). Notably, at 699.5 °C, the residual mass was recorded as 36.33%.

The TG and DTG curves of contaminated lignin revealed four maximum decomposition peaks located at 218, 349, 380, and 409 °C, as well as weight losses at 95.2 °C (loss of 13.78%), 351.5 °C (loss of 4.81%), 473 °C (loss of 14.24%), and 699.4 °C, with a residual mass of 52.96%, as seen in Figure 10(b).

According to TG/DTG analysis, the samples demonstrated thermal stability up to approximately 189 °C (unmodified lignin) and 182 °C (contaminated lignin), respectively. The subsequent steps were associated with their decomposition. The initial decomposition process at low temperatures is associated with water loss, followed by the decomposition of systems and the loss of structural water. The weight loss in the residual mass range corresponds to the thermal decomposition profile of lignin materials. The thermostability of lignin is associated with structural (syringyl/guaiacyl ratio) and functional (carbonyl, aromatic, and aliphatic hydroxyl groups) characteristics.[60] The difference in the remaining mass residues (from 36.33% for unmodified lignin to 52.96% for contaminated lignin), as shown in Figure 10(a) and 10(b), confirms the retention of Mo(VI) in the pores of Sarkanda grass lignin.

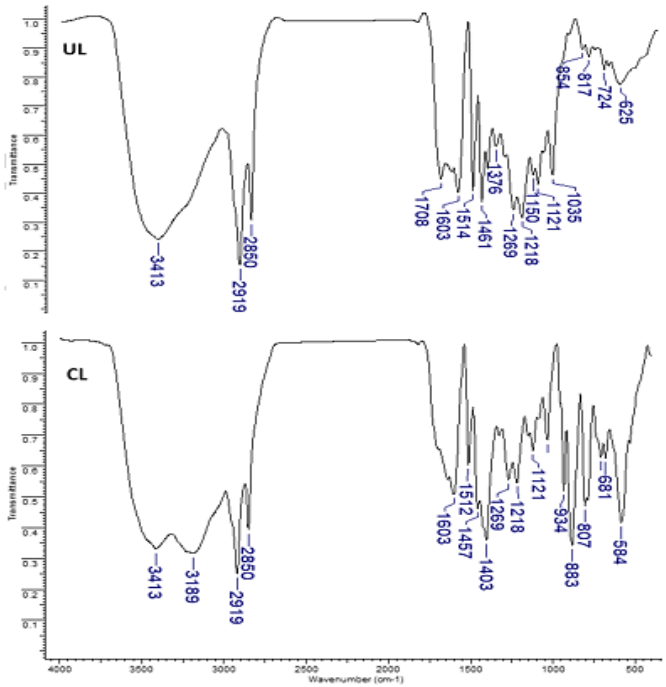

Figure 9: FTIR spectra for Sarkanda grass lignin before adsorption (UL) and after Mo(VI) adsorption (CL), contact time 60 min

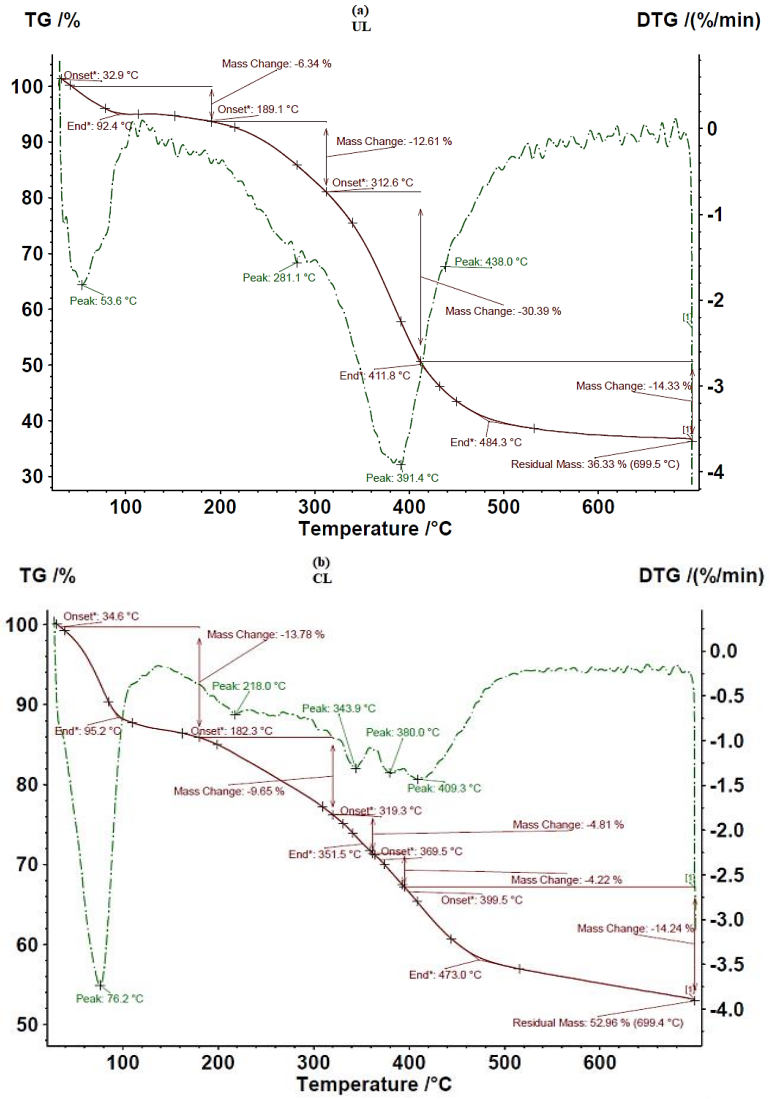

Figure 10: Thermogravimetric (red) and differential thermogravimetric (green) curves of Sarkanda grass lignin before (a) and after (b) Mo(VI) adsorption at a contact time of 60 min

Biostability

Molybdenum toxicity in plants is uncommon but does occur, causing symptoms similar to iron or copper deficiencies, including chlorosis, marginal leaf scorching, impaired nitrogen fixation, and reduced growth. Understanding the dynamics of molybdenum within culture medium–plant systems is essential for assessing its optimal availability and managing potential toxicity.[61]

Biostability studies have been conducted to assess the efficiency of lignin adsorption and the toxic effect of molybdenum on selected *Brassica oleracea* L. seeds. These parameters were monitored over a period of seven days in lignin samples contaminated with Mo(VI). As illustrated in Figure 11, the mean number of cabbage seeds germinated after three days was recorded for three replicates for the samples contaminated with Mo(VI). Similarly, the mean number of seeds germinated at three and seven days was documented for the filtrates resulting from Mo(VI) retention at the designated contact times (30, 60 and 90 minutes).

As illustrated in Figure 11, the inhibitory effect of Mo(VI) on the germination of cabbage seeds is evident, with an enhancement observed in the presence of elevated metal ion concentrations and prolonged contact times between the phases, thereby intensifying the abiotic stress. Therefore, in the study involving 20 seeds, it was observed that the control samples (lignin and distilled water) exhibited an average germination rate of 95%, while the filtrates demonstrated an almost equivalent germination rate of 95% after 3 days and 7 days, respectively. However, for a contact time of 30 minutes, the germination rate decreased by nearly 10%, reaching 86%. This finding indicates that a longer contact

time is necessary to achieve adsorption equilibrium, which is consistent with the experimental hypothesis derived from the analysis of thermokinetic data.

In lignin samples contaminated with aqueous solutions containing Mo(VI) concentrations of up to 76.752 mg/L at a contact time of 30 minutes, germinated seeds were observed after 3 days. The number of seeds observed was acceptable, as expected. However, seven days after germination, all contaminated lignin samples exhibited no further germination, regardless of contact time or Mo(VI) concentration. The existing seedlings did not evolve and actually perished. This phenomenon is attributed to the effective adsorption of Mo(VI) in the pores of Sarkanda grass lignin, which is thus a promising candidate for the eco-adsorbent category.

As illustrated in Table 4, a thorough examination of the experimental data regarding the energy and germination capacity reveals a remarkable synchronization with the number of germinated seeds, particularly evident in the case of filtrates and lignin samples contaminated with Mo(VI). Therefore, the adsorption non-equilibrium state is confirmed for the 30-minute contact time, where the filtrates are more concentrated and the germination energy is less intense, compared to the experimental indices checked at 60 and 90 minutes, where the filtrates are more diluted as a result of the more accentuated retention of Mo(VI) in the lignin pores.

In the case of contaminated lignin, the increase in molybdenum concentration and contact time induce a decrease in the germination energy to zero values at all three contact times, in the concentration range of 76.752-95.94 mg/L of Mo(VI) (Table 4).

The germination capacity of lignin contaminated with Mo(VI) was negligible in all cases, while the filtrates exhibited a variation similar to the germination energy, with values close to those observed in the control sample and independent of the Mo(VI) concentration. Negligible differences were observed for contact times of 60 and 90 minutes (Table 4), suggesting that a 60-minute contact time is optimal for achieving an efficient adsorption equilibrium of Mo(VI) on Sarkanda grass lignin. This conclusion is further supported by the morphological, thermal, thermodynamic, and kinetic analyses conducted.

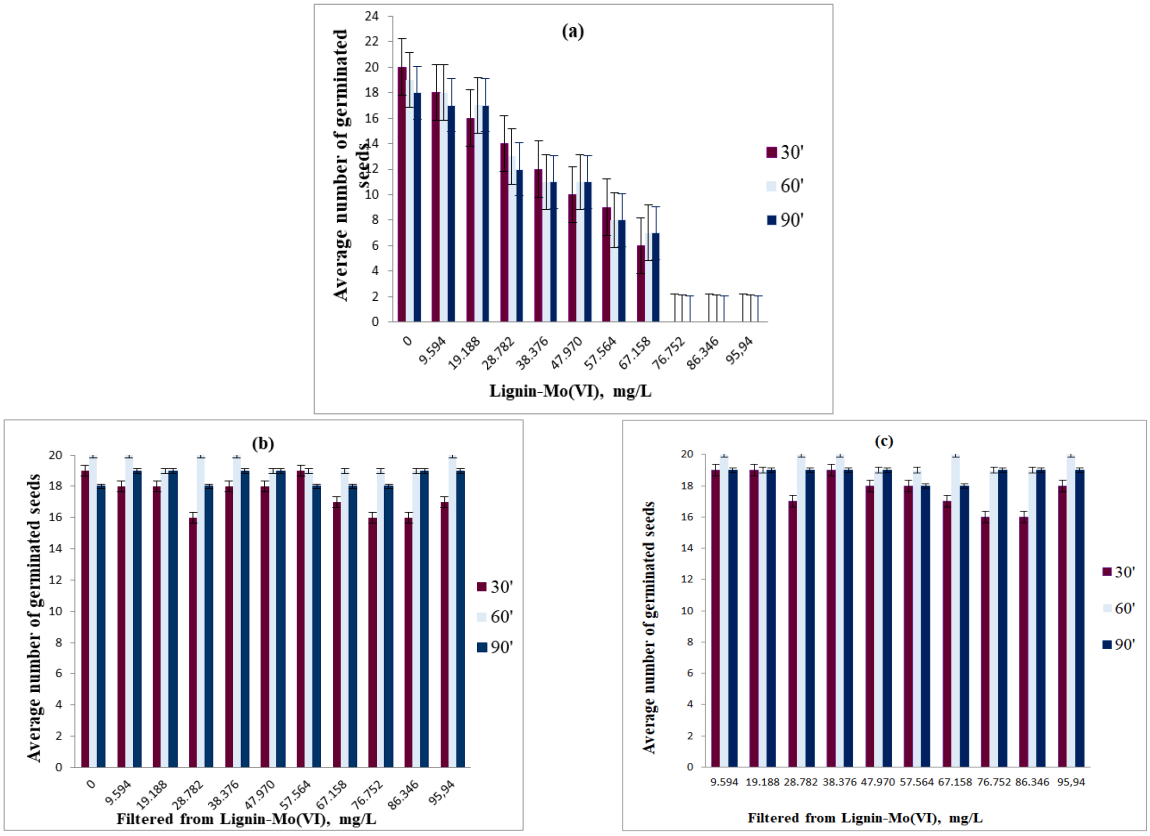

Figure 11: Average number of *Brassica oleracea L.* seeds germinated after 3 days of contact with contaminated samples (a), and after 3 days (b) and 7 days (c) of contact with the filtrates resulting from Mo(VI) adsorption

Table 4
Mean values of germination energy and capacity of seeds in contact with contaminated samples and the filtrates resulting from Mo(VI) adsorption for various contact times between the phases

Lignin/Mo(VI) (mg/L)	Contact time (min)						Lignin/Mo(VI) (mg/L) filtered	Contact time (min)					
	30	60	90	30	60	90		30	60	90	30	60	90
	Eg,%			Fg,%				Eg,%			Fg,%		
0	100	95	90	100	95	90	0	95	100	90	95	100	95
9.594	90	90	85	0	0	0	9.594	95	100	95	95	100	95
19.188	80	85	85	0	0	0	19.188	80	95	95	95	95	95
28.782	70	65	60	0	0	0	28.782	80	100	90	85	100	95
38.376	60	55	55	0	0	0	38.376	90	100	95	95	100	95
47.970	50	55	55	0	0	0	47.970	90	95	95	90	95	95
57.564	45	40	40	0	0	0	57.564	95	95	90	90	95	90
67.158	30	35	35	0	0	0	67.158	85	95	90	85	100	90
76.752	0	0	0	0	0	0	76.752	80	95	90	80	95	95
86.346	0	0	0	0	0	0	86.346	80	95	95	90	95	95
95.94	0	0	0	0	0	0	95.94	85	100	95	90	100	95

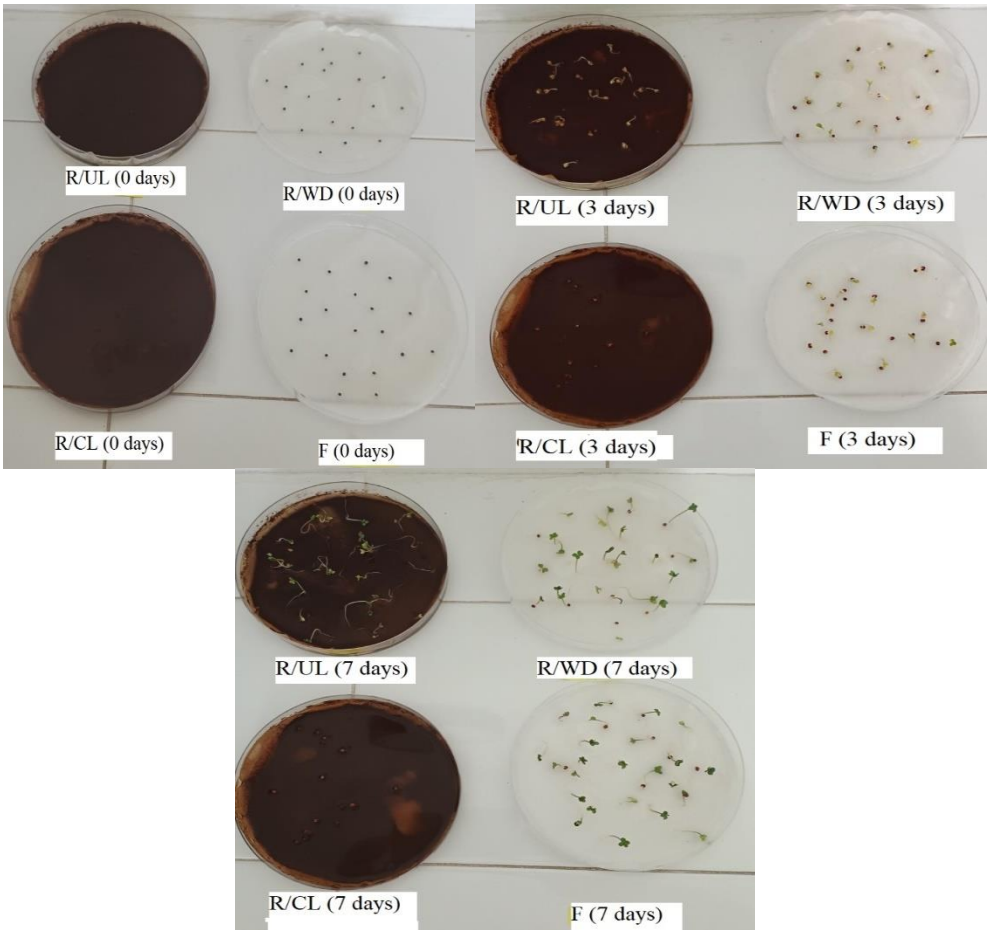

Figure 12: Germination of *Brassica oleracea* L. seeds over a period of 7 days in contact with contaminated samples (adsorption time of 60 min and a concentration of 95.94 mg/L Mo(VI))

As illustrated in Figure 12, the germination of *Brassica oleracea* L. seeds was monitored over the course of one week. The experimental conditions included reference/uncontaminated lignin (R/UL), lignin contaminated with Mo(VI) (CL), reference/distilled water (R/DW), and the filtrate (F) obtained after adsorption for 60 minutes at a concentration of 95.94 mg/L Mo(VI).

The reproducibility of observations concerning morphological and compositional analyses, in conjunction with kinetic, chemical equilibrium, thermostability, and biostability data, recommend lignin from Sarkanda grass as a viable alternative for Mo(VI) retention under static conditions in

aqueous environments. This is supported by the chemical reactivity and availability of lignin to engage in ion exchanges and chelation, in addition to its heterogeneous and porous structure, which is characterized by cavities that augment the surface area available for adsorption. The economic viability of lignin is substantiated by its regenerability, abundance, its quality as a biomass by-product, and the relatively easy processing. Furthermore, its ecological characteristics, such as biodegradability, require prioritized research on optimizing polycyclic regeneration conditions, with the aim of achieving scalability.[14]

CONCLUSION

Lignin, a biomass fraction that is underutilized, possesses a variety of functional groups available for deprotonation. This property renders it a potential chelating agent for metal ions, such as Mo(VI), and implicitly a favorable adsorption agent under static conditions. The present study demonstrates the efficacy of Sarkanda grass lignin as an adsorbent for Mo(VI) from contaminated aqueous environments under precisely established experimental conditions (temperature: 20 ± 0.1 °C, pH 5.7, both for lignin and for aqueous solutions of the polluting species), a dose of 5 g adsorbent/L pollutant solution, a concentration range of 9.594–95.94 mg/L Mo(VI), and an interphase contact time of 60 minutes.

The R^2 correlation coefficients, which are instrumental in evaluating the efficiency of an adsorbent from a pragmatic standpoint, as deduced from the experimental Freundlich and Langmuir adsorption isotherms, serve to indicate the probability of chemisorption in the polylayer. Consequently, the Freundlich model emerges as a more suitable model for describing the retention of Mo(VI) from aqueous media on Sarkanda grass lignin. Furthermore, the thermodynamic parameters are in full agreement with the conclusion drawn from the interpretation of the experimental isotherms. This demonstrates the spontaneous, thermodynamically favorable, partially disordered, and possibly endothermic character of the adsorption. This is expressed by the increase in entropy and enthalpy, and respectively by the decrease in Gibbs free energy. This thermodynamic behavior is similar to that encountered in already established adsorbents.

From a kinetic perspective, the pseudo-II order Ho-McKay model exhibited a superior capacity to describe the adsorption of Mo(VI) from aqueous media on Sarkanda grass lignin when compared to the pseudo-I order Lagergren model. This observation was confirmed by the (R^2) correlation coefficients, which reached unity in all cases. This finding suggests the presence of electrostatic interactions between the participating species and is consistent with the conclusions drawn for the Freundlich model. The Freundlich model posits the likelihood of chemical adsorption, attributing this phenomenon to the emergence of semiionic bonds, which subsequently leads to the formation of relatively stable lignomolybdenum complexes.

The results of the SEM, EDX, and FTIR analyses indicated the absorption of Mo(VI) from an aqueous medium and the post-adsorption morphological changes on the surface of Sarkanda grass lignin. These findings were corroborated by TG-DTG analyses, which demonstrated the efficiency of lignin as an adsorbent for the studied metal species by showing a difference in mass residues (36.3% for unmodified lignin and 52.96% for contaminated lignin).

The adsorption capacity of Sarkanda grass lignin was also assessed by performing bioassays on *Brassica oleracea* L. seeds, which were incorporated into lignin contaminated with Mo(VI) at concentrations ranging from 9.594 to 95.94 milligrams per liter of Mo(VI). These bioassays were performed on the filtrates resulting from the separation of the two post-adsorption phases at three different interphase contact times. The germination tests and the evaluated biological parameters highlighted the efficient detoxification of the aqueous phase (filtered, without toxic potential) and implicitly the retention of Mo(VI) in the lignin pores, clearly deduced from the toxicity of the contaminated lignin. Therefore, it can be concluded that Sarkanda grass lignin is an ecologically sustainable adsorbent.

Experimental data demonstrate the potential of Sarkanda grass lignin as an adsorbent for the removal of Mo(VI) from contaminated aqueous environments. The adsorption capacity of lignin is noteworthy, and its attributes as a biomaterial, including its renewability and biodegradability, make it a viable option. Additionally, lignin is a cost-effective resource, a secondary product that is abundant and can be valorized for various agro-industrial applications. Its scalability is a key advantage, and the exploration of efficient regeneration methods, such as acid/base treatment, electrochemical

regeneration, and the use of ecological solvents, is crucial for ensuring sustainability. These techniques are currently under research to align with the current trend of economic biocircularity.

Furthermore, to overcome the limitations of rapid superficial complexation observed in raw lignin, future research should focus on its structural modification. Techniques such as electrospinning lignin into nanofibers or grafting it onto high-surface-area templates are currently under investigation to expand the internal pore network and optimize polycyclic regeneration conditions, with the aim of achieving scalability.

ACKNOWLEDGEMENT: The authors declare no specific funding for this work.

REFERENCES

[1] S. Mitra, A. J. Chakraborty, A. M. Tareq, T. B. Emran, F. Nainu *et al*., *J. King Saud Univ. Sci*., **34**, 101865 (2022), https://doi.org/10.1016/j.jksus.2022.101865
[2] T. S. Khayyun and A. H. Mseer, *Appl. Water. Sci*., **9**, 170 (2019), https://doi.org/10.1007/s13201-019-1061-2
[3] D. G. Barceloux, *J. Toxicol. Clin. Toxicol*., **37**, 231 (1999), https://doi.org/10.1081/CLT-1000102422
[4] Y. H. Huang, C. Tang and H. Zeng, *Chem. Eng. J*., **200**, 257 (2012), https://doi.org/10.1016/j.cej.2012.06.047
[5] J. A. Novotny, *J. Evid. Compl. Alt. Med*., **16**, 64 (2011), https://doi:10.1177/2156587211406732
[6] C. W. Wang, C. Liang and H. J. Yeh, *Chemosphere*, **147**, 82 (2016), https://doi.org/10.1016/j.chemosphere.2015.12.052
[7] D. Kim, J. Lee and J. Seo, *Catalysts*, **11**, 217 (2021), https://doi.org/10.3390/catal11020217
[8] X. Wang, C. Liu, A. Wang, J. Liu and X. Jia, *Multipurp. Util. Miner. Resour*., **45**, 69 (2024), https://doi.org/10.3969/j.issn.1000-6532.2024.04.010
[9] M. L. C. M. Henckens, P. P. J. Driessen and E. Worrell, *Resour. Conserv. Recycl*., **134**, 61 (2018), https://doi.org/10.1016/j.resconrec.2018.03.002
[10] E. Ungureanu, B. M. Tofanică, O. C. Ungureanu, M. E. Fortună, R. Rotaru *et al*., *Cellulose Chem. Technol*., **59**, 451 (2025), https://doi.org/10.35812/CelluloseChemTechnol.2025.59.40
[11] F. G. Ávila, J. Cabrera-Sumba, S. Valdez-Pilataxi, J. Villalta-Chungata, L. Valdiviezo-Gonzales *et al*., *Clean. Eng. Technol*., **24**, 100879 (2025), https://doi.org/10.1016/j.clet.2025.100879
[12] M. S. Aktar, M. S. R. Shakil and F. Tuj-Zohra, *Clean. Eng. Technol*., **17**, 100687 (2023), https://doi.org/10.1016/j.clet.2023.100687
[13] A. Khosravi, M. Javdan, G. Yazdanpanah and M. Malakootian, *Appl. Water Sci*., **10**, 1 (2020), https://doi.org/10.1007/s13201-020-01257-5
[14] E. Ungureanu, B. M. Tofanică, E. Ulea, O. C. Ungureanu, M. E. Fortună *et al*., *Polymers*, **17**, 2263 (2025), https://doi.org/10.3390/polym17162263
[15] Z. Yang, X. Wan, Y. Chen, X. Chen, Z. Wang *et al*., *J. Environ. Chem. Eng*., **13**, 119080 (2025), https://doi.org/10.1016/j.jece.2025.119080
[16] E. Ungureanu, "Lignin, Aromatic Natural Polymer with High Potential for Recovery", Pim Press, Iasi, 2011, http://www.pimcopy.ro/editura/
[17] B. Du, L. Chai, Q. Zheng, Y. Liu, X. Wang, *et al*., *Int. J. Biol. Macromol*., **234**, 123668 (2023), https://doi.org/10.1016/j.ijbiomac.2023.123668
[18] N. Ayawei, A. N. Ebelegi and D. Wankasi, *J. Chem*., **2017**, 11 (2017), https://doi.org/10.1155/2017/3039817
[19] T. S. Khayyun and A. H. Mseer, *Appl. Water Sci*., **9**, 170 (2019), https://doi.org/10.1007/s13201-019-1061-2
[20] E. Ungureanu, M. E. Fortună, D. C. Țopa, C. O. Brezuleanu, O. C. Ungureanu *et al*., *Polymers*, **15**, 3794 (2023), https://doi:10.3390/polym15183794
[21] E. D. Revellame, D. L. Fortela, W. Sharp, R. Hernandez and M. E. Zappi, *Clean. Eng. Technol*., **1**, 100032 (2020), https://doi.org/10.1016/j.clet.2020.100032
[22] A. Mohrazi, R. Ghasemi-Fasaei, A. Mojiri and S. Safarzadeh, *Sci. Rep*., **14**, 13225 (2024), https://doi.org/10.1038/s41598-024-64130-4
[23] X. Shu, Y. Wu, X. Zhang and F. Yu, *Appl. Clay Sci*., **260**, 107494 (2024), https://doi.org/10.1016/j.clay.2024.107494
[24] Z. Yang, X. Wan, Y. Chen, X. Chen, Z. Wang *et al*., *J. Environ. Chem. Eng*., **13**, 119080 (2025), https://doi.org/10.1016/j.jece.2025.119080
[25] X. Liu, J. Lu, X. Fang, J. Zhou and Q. Chen, *Chemosphere*, **308**, 136374 (2022), https://doi.org/10.1016/j.chemosphere.2022.136374
[26] A. Pui and D. Cozma, "Basics of Coordination Compound Chemistry", Matrix Rom Press, Iasi, 2003
[27] U. Madan and L. R. Kakkar, *Talanta*, **29**, 623 (1982), https://doi.org/10.1016/0039-9140(82)80013-1)
[28] J. Wang and X. Guo, *Chemosphere*, **258**, 127279 (2020), https://doi.org/10.1016/j.chemosphere.2020.127279
[29] S. K. Pereira, S. Kini, B. Prabhu and G. P. Jeppu, *Appl. Water. Sci*., **13**, 29 (2023), https://doi.org/10.1007/s13201-022-01800-6

[30] H. R. Ahmed, K. F. Kayani, A. M. Ealias and K. H. H. Aziz, *Water Air. Soil. Pollut.*, **236**, 346 (2025), https://doi.org/10.1007/s11270-025-07982-4
[31] K. H. Chong and B. Volesky, *Biotechnol. Bioeng.*, **47**, 451 (1995), https://doi.org/10.1002/bit.260470406.
[32] S. Leveneur, *Can. J. Chem. Eng.*, **101**, 7078 (2023), https://doi.org/10.1002/cjce.24956
[33] A. Dąbrowski, *Adv. Colloid. Interface. Sci.*, **93**, 135 (2001), https://doi.org/10.1016/S00018686(00)00082-8
[34] Y. S. Ho and G. McKay, *Process Biochem.*, **34**, 451 (1999), https://doi.org/10.1016/S0032-9592(98)00112-5
[35] C. G. Boeriu, D. Bravo, R. J. A. Gosselink and J. E. G. van Dam, *Ind. Crop. Prod.*, **20**, 205 (2004), https://doi:10.1016/j.indcrop.2004.04.022
[36] A. Ali, N. Zhang and R. M. Santos, *Appl. Sci.*, **13**, 12600 (2023), https://doi.org/10.3390/app132312600
[37] M. E. Fortuna, E. Ungureanu, R. Rotaru, A. Bargan, O. C. Ungureanu *et al.*, *Polymers*, **15**, 4731 (2023), https://doi.org/10.3390/polym15244731
[38] C. Li, S. Feng, Y. Shao, L. Jiang, X. Lu *et al.*, *J. Environ. Sci.*, **19**, 725 (2007), https://doi.org/10.1016/s1001-0742(07)60121-1
[39] E. Ungureanu, A. E. Trofin, L. C. Trincă, A. M. Ariton, O. C. Ungureanu *et al.*, *Cellulose Chem. Technol.*, **55**, 939 (2021), https://doi.org/10.35812/CelluloseChemTechnol.2021.55.80
[40] M. Ahmaruzzaman, *Adv. Colloid. Interface. Sci.*, **166**, 36 (2011), https://doi.org/10.1016/j.cis.2011.04.005
[41] M. Wasilewska, A. Derylo-Marczewska and A. W. Marczewski, *Molecules*, **29**, 2038 (2024), https://doi.org/10.3390/molecules29092038
[42] A. Y. Kurmysheva, M. D. Vedenyapina, S. A. Kulaishin, P. Podrabinnik, N. W. S. Pinargote *et al.*, *Int. J. Mol. Sci.*, **24**, 8700 (2023), https://doi.org/10.3390/ijms24108700R
[43] J. Torres, L. Gonzatto, G. Peinado, C. Kremer and E. Kremer, *J. Solut. Chem.*, **43**, 1687 (2014), https://doi.org/10.1007/s10953-014-0231-y
[44] P. L. Smedley and D. G. Kinniburgh, *Appl. Geochem.*, **84**, 387 (2017), https://doi.org/10.1016/j.apgeochem.2017.05.008
[45] L. Molina-Calderón, C. Basualto-Flores, V. Paredes-García and D. Venegas-Yazigi, *Sep. Purif. Technol.*, **299**, 121708 (2022), https://doi.org/10.1016/j.seppur.2022.121708
[46] B. Brazesh, S. M. Mousavi, M. Zarei, M. Ghaedi, S. Bahrani *et al.*, *Interface Sci.*, **33**, 587 (2021), https://doi.org/10.1016/B978-0-12-818805-7.00003-5
[47] E. Ungureanu, C. Samuil, D. C. Țopa, O. C. Ungureanu, B. M. Tofanică *et al.*, *Crystals*, **14**, 381 (2024), https://doi:10.3390/cryst14040381
[48] I. Langmuir, *J. Am. Chem. Soc.*, **38**, 2221 (1916), https://doi.org/10.1021/ja02268a002
[49] H. M. F. Freundlich, *J. Phys. Chem.*, **57**, 385 (1906)
[50] N. Nasuha, B. H. Hameed, T. Azam and M. Din, *J. Hazard. Mater.*, **175**, 126 (2010), https://doi.org/10.1016/j.jhazmat.2009.09.138
[51] X. Zhou, X. Yu, R. Maimaitiniyazi, X. Zhang and Q. Qu, *Heliyon*, **10**, 28188 (2024), https://doi.org/10.1016/j.heliyon.2024.e28188
[52] S. Li, Y. Li, S. Deng, X. E. Cao and K. B. Lee, *Energy*, **329**, 136846 (2025), https://doi.org/10.1016/j.energy.2025.136846
[53] J. M. C. Menezes, A. M. da Silva Bento, J. H. da Silva, F. J. de Paula Filho, J. G. M. da *Costa et al.*, *Chemosphere*, **261**, 128144 (2020), https://doi.org/10.1016/j.chemosphere.2020.128144
[54] Y. T. da Costa Santos, S. Salvestrini, C. B. G. Vieira, J. M. C. Menezes, A. J. A. Ribeiro *et al.*, *Environ. Sci. Pollut. Res.*, **31**, 61740 (2024), https://doi.org/10.1007/s11356-024-35194-6
[55] E. C. Lima, A. A. Gomes and H. N. Tran, *J. Molec. Liq.*, **311**, 113315 (2020), https://doi.org/10.1016/j.molliq.2020.113315
[56] U. A. Edet and A.O. Ifelebuegu, *Processes*, **8**, 665 (2020), https://doi.org/10.3390/pr8060665
[57] S. Pasieczna-Patkowska, M. Cichy and J. Flieger, *Molecules*, **30**, 684 (2025), https://doi.org/10.3390/molecules30030684
[58] S. G. Kostryukova, H. B. Matyakubov, Y. Y. Masterova, A. Sh. Kozlov, M. K. Pryanichnikova *et al.*, *J. Anal. Chem.*, **78**, 718 (2023), https://doi.org/10.1134/S1061934823040093
[59] S. Sadighi, S. Kamal and M. Targhi, *Bull. Chem. React. Eng. Catal.*, **12**, 49 (2017), https://doi.org/10.9767/bcrec.12.1.486
[60] A. M. Ariton, Ș. Creanga, L. C. Trinca, S. I. Bors, E. Ungureanu *et al.*, *Cellulose Chem. Technol.*, **49**, 765 (2015), https://www.cellulosechemtechnol.ro/pdf/CCT9-10(2015)/p.765-774.pdf
[61] M. Rana, N. K. Sankhyan, P. Thakur, B. Bhawna, A. Anjali *et al.*, *Discov. Soil.*, **2**, 89 (2025), https://doi.org/10.1007/s44378-025-00118-4
[62] B. M. Tofanica, E. Ungureanu, O. C. Ungureanu, M. E. Fortuna, I. Volf *et al.*, *Bul. Inst. Polit. Iasi*, **70**, 33 (2024), https://doi.org/10.5281/zenodo.14582064